WP9: Quantum supercomputer simulations

1. Major activities and results

<u>Task 9.1</u> Correlated quantum dynamics.

A typical manifestation of the quantum many-body effects is the electron correlation which results from the Coulomb and exchange interactions between the electrons combined with the underlying quantum non-locality. Since in general the electron correlation reshapes the probability density in configuration space, it is difficult to elucidate this effect for higher dimensions. Therefore, to better understand the effects of electron correlation in atoms and molecules one needs, besides one-particle quantities such as the electron density function, to consider also extensions which explicitly incorporate many-body effects. Such an appropriate quantity is the electronic pair density function which represents the probability density of finding two electrons at distance **u** from each other:

$$I(\mathbf{u},t)=\left\langle \Psi(\mathbf{R},t)\left|\sum_{i<j}\delta\left[\left(\mathbf{r}_i-\mathbf{r}_j\right)-\mathbf{u}\right]\right|\Psi(\mathbf{R},t)\right\rangle \quad ,$$

where $\mathbf{r}_i$ is the position of the *i*th electron and the many-body wave function $\Psi(\mathbf{R},t)$ resides in configuration space.

The importance of the electron pair density comes from the fact that it can be associated with experimental data obtained from x-ray scattering, and it can also be used to visualize the notion of exchange and correlation holes which surround the quantum particles.

Here in this report we calculate the electron pair densities for helium atom in 2 ^{1}S and 2 ^{3}S states using the recently proposed time-dependent quantum Monte Carlo (TDQMC) method which employs sets of particles and quantum waves to describe the ground state and the time evolution of many-electron systems. In TDQMC each electron is described statistically as an ensemble of walkers which represent different replicas of that electron in position space, where each walker is guided by a separate time-dependent de Broglie-Bohm pilot wave. The correlated guiding waves obey a set of coupled time-dependent Schrödinger equations (TDSE) where the electron-electron interactions are accounted for using explicit non-local Coulomb potentials. The large speed up of the calculations when using TDQMC comes from the fact that walker's distribution reproduces the amplitude (or modulus square) of the many-body wave function while its phase is being disregarded as it is not needed for most applications. Also, the TDQMC method can be implemented very efficiently on parallel computers where tens of thousands of coupled Schrödinger equations can be solved concurrently for affordable time. Our results for the electron-pair density of helium as well as the following coulomb and exchange holes are shown in figure 1. These results were published in paper IC_13.

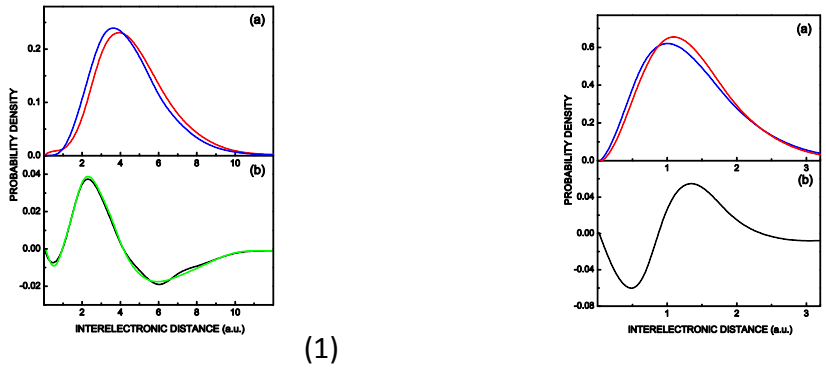

(1) (2)

Фиг.1 Electron pair density as function of the distance between the electrons for orthohelium (1) and parahelium (2).

Task 9.3: Maximal hydrogen loading of transition metal clusters in gas phase and on support

Theoretical investigation of the interaction of H_2O with CeO_x ($x \leq 2$)

A slab consisting of two O-Ce-O trilayers with a stripe of a single O-Ce-O trilayer atop was used to represent a step edge running along the $\langle 2\bar{1}\bar{1} \rangle$ direction on the (111) surface plane (see Figure 1a; the other panels of Figure 1 display the structures of all studied adsorption complexes **b - m**). The adsorption of water, estimated by the adsorption energy, $E_{ad}(H_2O)$, at the terrace, site **b**, and at the step, site **c**, is exothermic, suggesting that both sites can be populated upon water adsorption. For the site **b** we obtained $E_{ad}(H_2O) = -0.50$ eV. At the step site **c** the water molecule is more strongly bound by 0.39 eV, amounting to $E_{ad}(H_2O) = -0.89$ eV.

In addition to molecular adsorption, we also considered heterolytic dissociation of H_2O at terraces, sites **d** and **e**, and step edges, sites **f** – **h**, on stoichiometric $CeO_2(111)$. We found that dissociated water at terrace sites is less stable than intact adsorbed molecule by 1.14 eV or by 0.21 eV (in agreement with Fronzi et al.[1] depending on the adsorption site **d** or **e**, respectively. In contrast, the dissociation at steps becomes favorable for configurations **f** ($E_{ad}(H_2O) = -1.21$ eV) and **g** ($E_{ad}(H_2O) = -1.14$ eV) by 0.32 and 0.25 eV, respectively. In the most stable configuration, the released proton forms an OH group with 2–fold coordinated oxygen, while the OH^- remains 1–fold coordinated to one of the Ce^{4+} ions. The O–H vibrational frequency of the 2–fold OH group, 3762 cm^{-1}, (*2736* cm^{-1}; here and in the following the corresponding calculated O-D stretching frequencies are given in italics), is close to that of the isolated one **i**, while the frequency of the 1-fold group is calculated to be about 50 cm^{-1} higher.

According to Fronzi et al.,[1] formation of hydroxyl groups from water on reduced CeO_{2-x}, can be modeled as adsorption of hydrogen atoms on stoichiometric ceria. In each of our models, shown in Figure 1, configurations **i** – **m,** the hydroxyl group was produced by attachment of a single H atom at the corresponding surface O center; concomitantly, one of the surface Ce^{4+} ions in proximity of the OH group is reduced to Ce^{3+} (labeled in blue in Figure 1).

Attachment of H to a 3-fold O center in the configurations **l** and **m** provides stabilization (computed with respect to ½ H_2) by –0.76 and –0.70 eV, respectively. The corresponding OH groups do not form hydrogen bonds with nearest oxygen ions. On the contrary, the 3–fold OH groups in the proximity of the step form weak hydrogen bonds with nearest oxygen ions, configurations **j** and **k**, which are stabilized by –0.89 eV. Thus, one can estimate the energy of these hydrogen bonds to be 0.1 – 0.2 eV.

---

[1] Fronzi, M.; Piccinin, S.; Delley, B.; Traversa, E.; Stampfl, C. *Physical Chemistry Chemical Physics* **2009**, *11*, 9188-9199.

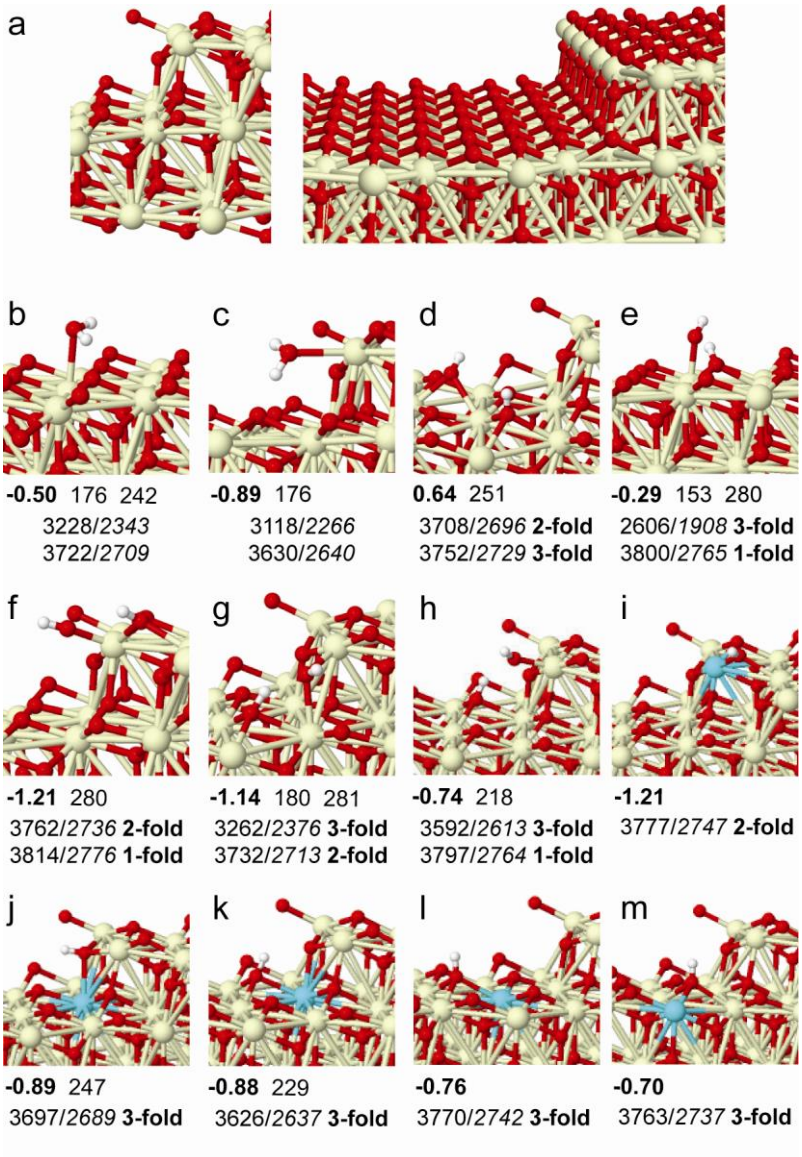

Fig. 1. Sketches of the optimized models of the stepped CeO_2(111) surface - (**a**) bare surface, the surface with one intact (**b-c**) or dissociated (**d-h**) adsorbed water molecule (surface OH groups) or adsorbed hydrogen atom (**i-m**). Below each panel are displayed: adsorption energy of H_2O (**b-c**), dissociation energy of H_2O with respect to gas-phase molecule (**d-h**), adsorption energy of H with respect to ½ H_2 in gas phase (**i-m**), in eV (all the numbers are in bold); the length of hydrogen bonds (if formed; next to the energy values), in pm; calculated stretching O-H/*O-D* vibrational frequencies (bottom line), in cm^{-1}. Color coding: Ce^{4+} – yellow, Ce^{3+} – blue, O – red, H – white.

The hydroxyl group at the 2–fold coordinated oxygen at the step, site **i**, stabilized by –1.21 eV, is found to be the most favorable energetically. It suggests preferential formation of the 2–fold hydroxyls over the 3–fold ones.

The study was performed by H. Aleksandrov, P. Petkov and G. Vayssilov

<u>Task 9.4: Metal-support interaction</u>

Adsorption of CeO_2 units on Al_2O_3(100) surface

We perform periodic calculations using a slab model of $Al_2O_3(100)$ surface. Our preliminary calculations are done using relatively small model consisting of four layers of Al and O atoms (totally 80 atoms); the bottom layer is fixed at bulk optimized positions. The pure surface $Al_2O_3(100)$, is stepped-like and has parts: "low part" and "top part" (Figure 2).

We have modeled various structures with adsorbed 1 - 6 CeO_2 units on $Al_2O_3(100)$ (part of them are shown in Figure 3). Our preliminary results show that formations of CeO_2 species on Al_2O_3 are unstable with respect to CeO_2 and Al_2O_3 slab models (Table 1), (binding energies of CeO_2 units are positive). In all cases CeO_2 units prefer to be located at the low part of the $Al_2O_3(100)$ surface. CeO_2 units are most stable separately; $(CeO_2)_3$ structures ordered in a line or in a triangle form are less stable by 0.32 and 0.65 eV, respectively compared to the isolated CeO_2 species (Table 1). In the structures where CeO_2 are positioned in a line, CeO_2 units prefer to form dimers during the geometry optimization. In general, we noticed that adsorption of CeO_2 units causes notable deformation of Al_2O_3 support. Further investigations are necessary in order to quantify this effect.

Table 1. Average binding energy (in eV) of CeO_2 units with respect to the $(CeO_2)_{54}$ slab model on $Al_2O_3(100)$:
$BE(CeO_2) = \{E[(CeO_2)_N/Al_2O_3(100)] - E[Al_2O_3(100)] - N*E[(CeO_2)_{54}]/54\}/N$; N = 1 - 6

Structure	**N**	**BE(CeO_2)**
at_top_part	1	3.88
at_low_part	1	1.27
at_top_part_2_CeO2	2	3.17
triangle_at_low	3	1.92
triangle_at_top	3	2.18
line_at_low_part	3	1.59

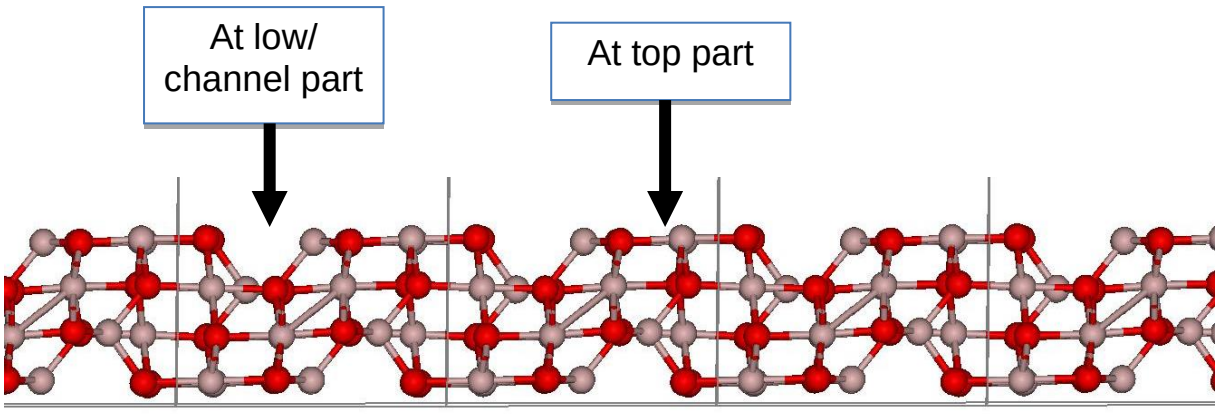

Fig. 2. $Al_2O_3(100)$ surface model. "Low part" and "top part" are indicated.

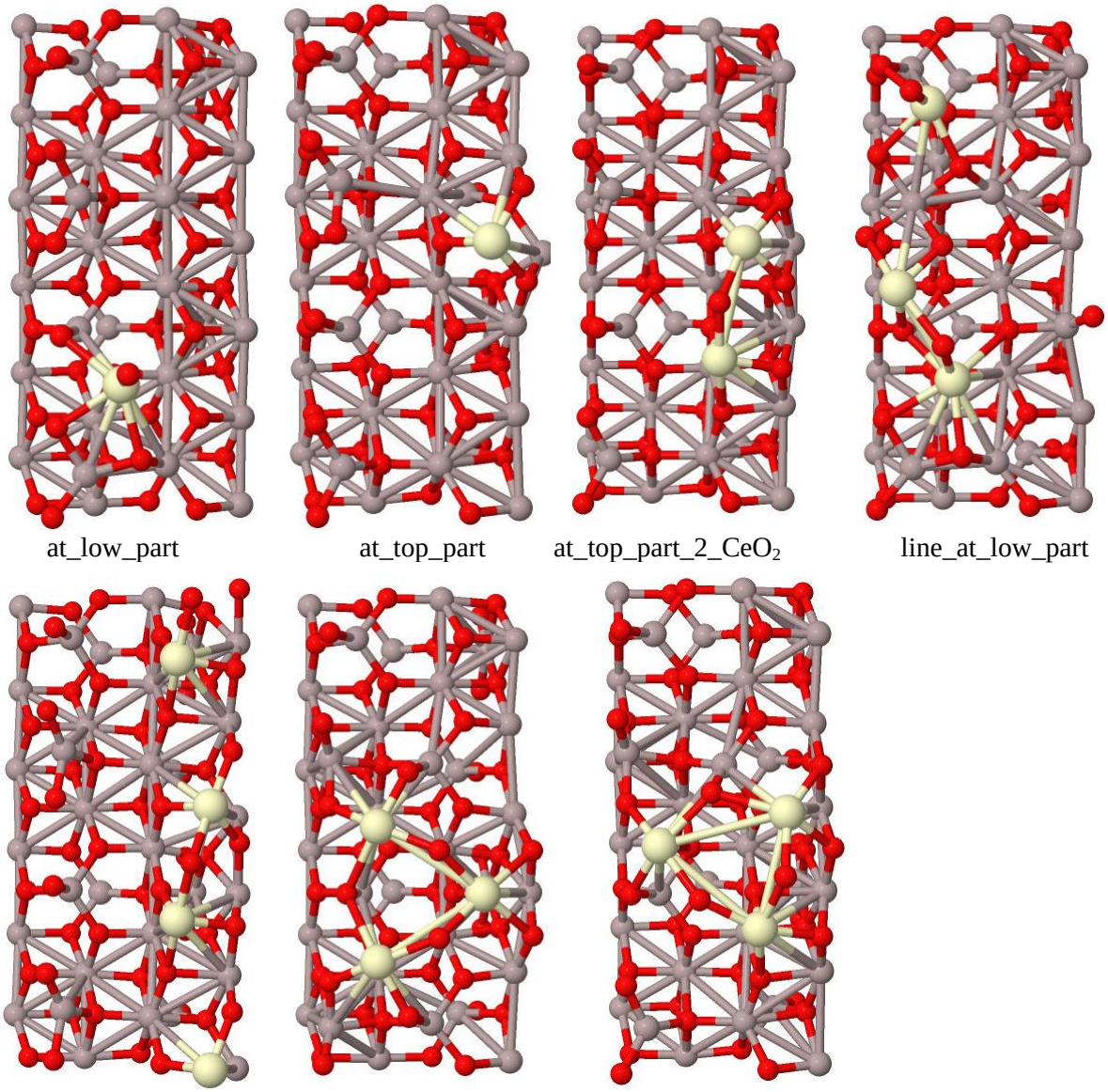

Fig. 3. Selected optimized models of $(CeO_2)_N/Al_2O_3(100)$ systems (N = 1-4). Color notation: O – red; Al – brown; Ce – yellow.

The study was performed by H. Aleksandrov and G. Vayssilov

<u>Task 9.5: Sorption of hydrogen and other small molecules in MOFs</u>

Quantum chemical modeling of hiper-fine coupling constant and EPR parameters in metal-organic frameworks with Cu^{2+}/Zn^{2+} dimers after adsorption of CO and CO_2.

Metal-organic frameworks are porous coordination polymers gained high interest in recent years because of their potential applications in many industrial processes. Especially the desired storage and separation of the "greenhouse gas" CO_2 induced many experimental and theoretical studies focused on the exceptional adsorption properties of metal-organic frame-works.

The hyperfine coupling constants (hfc) for 13C were obtained with single-point calculations using the optimized structures of the complexes at B3LYP level.49 Hfc for 13C were calculated on

grounds of DFT, employing the gradient-corrected exchange!correlation functional PBE,50 a triple-adzeta basis set with polarization functions.51 Relativistic effects have been included by the zero-order relativistic approximation (ZORA) and spin - orbit corrections. The calculations of the hfc constants have been carried out with the ADF code. For an accurate calculation of the A-tensor, one needs a very large basis set in the core region, especially for heavy nuclei. Such large basis sets (jcpl basis set from ADF basis set library) were applied for Cu^{2+}, which are basis sets especially designed for EPR A-tensor and NMR spin-spin coupling calculations.

The carbon monoxide is coordinated linearly to the metal ion (Cu^{2+}) while the carbon dioxide molecule is tilted with respect to the Cu-Zn axis with angle of 22° (Fig. 4). The adsorption of CO does not affect considerably the structure of the paddle wheel unit as the Cu-O distances to the ligand are elongated by 0.01-0.03 Å. This is related to the symmetric coordination of CO along the C4 symmetry axis of the complex and the weak binding of the adsorbates to the Cu^{2+} ion. The calculated hf coupling constants for ^{13}C in the adsorbed CO agree well with the experimentally measured values. The ^{13}C hfc tensor was found to be axially symmetric with -1.71 MHz for the $A^{C}_{xx,yy}$ components, while the A^{C}_{zz} component was calculated to be 1.3 MHz. The calculated $A_{xx,yy}$ and A_{zz} components are lower by 0.29 and 0.19 MHz, respectively, than the experimentally measured values but represent the major characteristics of the tensor, axial symmetry, and dipolar hyperfine coupling of about 1 MHz, and negative isotropic hyperfine coupling (Table 1). The adsorption energy of CO_2 coordinated to the Cu^{2+} ion at a mixed Cu/Zn paddle wheel unit is slightly stronger (by 3 kJ mol^{-1}) than that of CO. However, the nearly free rotation of CO_2, imposes a higher zero-point energy resulting in slightly weaker binding. Due to the tilted coordination of CO_2 and lower symmetry of the complex, additional sets of calculations were performed. The maximum energy variation for rotation of CO_2 around Zn-Cu axis was estimated to be very low, about 2 kJ mol^{-1} for partially optimized structures and 6 kJ mol^{-1} for the structures without relaxed paddle wheel constituents. Taking into account such a disorder in the arrangement of the adsorbed CO_2 molecules, the components of 13C hfc tensor were estimated using different orientations of CO_2 around Cu-Zn axis, and the $A^{C}_{xx,yy}$ and A^{C}_{zz} components were calculated for five different orientations of CO_2 around Zn-Cu axis, where the CO_2 molecule is tilted toward Cu-O(btc) bond and the components of A- tensor were averaged over the five orientations.

Table 1: ^{13}C hyperfine coupling constatnts of $^{13}CO_2$ and ^{13}CO adsorbed on $Cu_{2.97}Zn_{0.03}(btc)_2$ MOF.

	$A^{13C}_{xx,yy}$	A^{13C}_{zz}	β	A^{13C}_{iso}	$T^{13C}_{\perp}$	$r_{Cu\cdots C}$
$^{13}CO_{2,\ ads.}$ (2)[a]	-0.6	1.0	25°	-0.060	0.533	3.34 Å
Calculated	-0.4[b]	0.9[b]	22°			3.27 Å
$^{13}CO_{ads.}$ (3)[a]	-2.0	1.5	0°	-0.833	1.167	2.57 Å
Calculated	-1.7	1.3	0°			2.42 Å

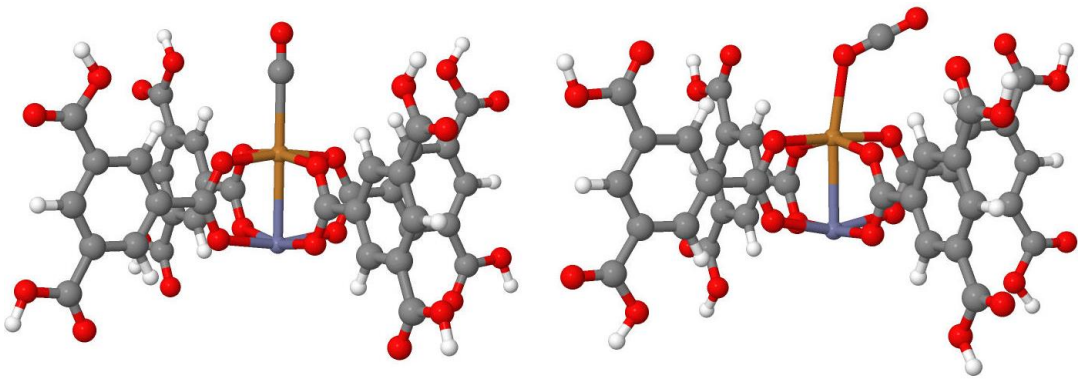

$CO/CuZn(BTC)_4$ complex $CO_2/CuZn(BTC)_4$ complex

Fig. 4. Optimized structures of the complexes with CO and CO_2. Gray color– C, red color– O, Ochre – Cu^{2+}, Blue color – Zn^{2+}

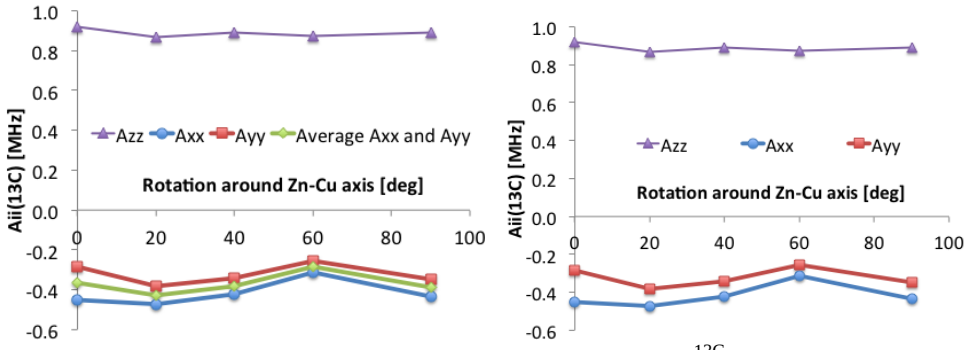

Fig. 5. Varuiation of the $A_{xx/yy}$ and A_{zz} components of A^{13C} tensor for CO_2, calculated for different orientations of CO_2 around Zn-Cu axes.

The computed ^{13}C hyperfine coupling tensors are slightly ortho-rhombic with $|A^{C}_{xx}-A^{C}_{yy}| <$ 0.13 MHz (Fig. 5). As it can be seen in Fig. 5, the A^{C}_{xx} and A^{C}_{yy} components are more sensitive to the position of CO2 around Cu-Zn axis while A^{C}_{zz} component of the ^{13}C from CO_2 remains almost unchanged during the rotation of CO_2.

The study was performed by Petko Petkov and Georgi Vayssilov

Computational modeling of the structure and properties of extra-framework gold ions in metal-organic frameworks

A metal-organic framework IRMOF-3 with incorporated gold (III) complex was investigated. After including of the complex the structure of the framework is changed and one of the carboxylate groups in the organic linker is rotated in order to avoid steric obstruction. Figure 6 represents the optimized structures of the IRMOF-3 framework before and after incorporating the gold (III) complex.

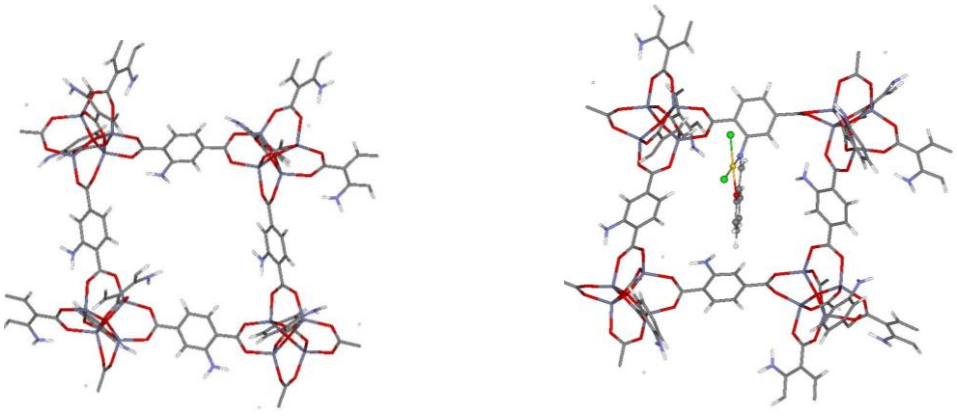

A **B**

Fig. 6. Optimized structure of IRMOF-3 before (A) and after incorporating the gold complex (B)

The interaction of the Au (III) ion with hydrogen was modeled as a part of the activation process in the hydrogenation reaction of alkenes. Two different types of heterolytic dissociative adsorption of hydrogen were investigated. The most stable structures are gained after reduction of the Au^{3+} cation to Au^{+} that leads to release of HCl molecule from the complex. The adsorption of hydrogen results in structures containing OH (L(OH)N-AuCl/HCl) or NH group (L(NH)O-AuCl/HCl), and these systems are with 158 and 203 kJ/mol more stable than the initial Au (III) complex. Figure 7 shows the optimized structures after interaction with hydrogen and release of HCl molecule.

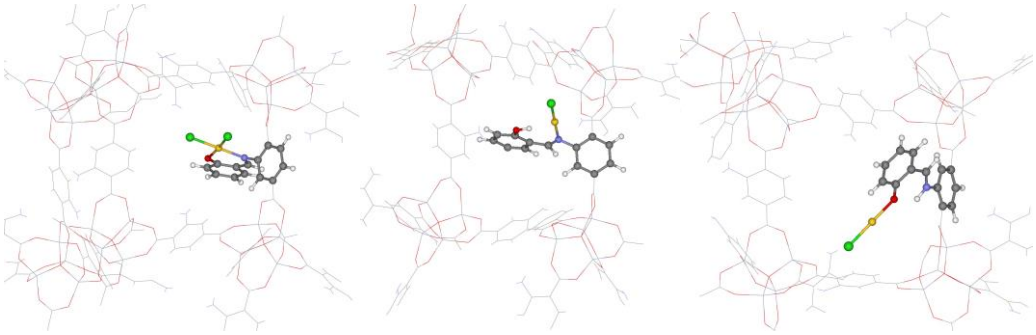

A **B** **C**

Fig. 7. Structure of the initial gold (III) complex (A) and the two most stable structures obtained after hydrogen adsorption and formation of OH (B) and NH (C) group

1. Publications related to the topic of the project, where the project is acknowledged DCVP 02/1

Published papers in scientific journals:

[IC_13] I. P. Christov, "Electron-pair densities with time-dependent quantum Monte Carlo", Journal of Atomic and Molecular Physics, vol.2013, Article ID 424570 (2013).

[GV_1] Y. Lykhach, V. Johánek, H. A. Aleksandrov, S. M. Kozlov, M. Happel, T. Skála, P. St. Petkov, N. Tsud, G. N. Vayssilov, K. C. Prince, K. M. Neyman, V. Matolín, J. Libuda "Water Chemistry on Model Ceria and Pt/Ceria Catalysts" The Journal of Physical Chemistry C, 116, 12103−12113 (2012). (IF = 4.81)

[GV_2] B. Jee, P. St. Petkov, G. N. Vayssilov, T. Heine, M. Hartmann, A. Pöppl "A Combined Pulsed Electron Paramagnetic Resonance Spectroscopic and DFT Analysis of the $^{13}CO_2$ and ^{13}CO Adsorption in the Metal-Organic Framework $Cu_{2.97}Zn_{0.03}(btc)_2$" The Journal of Physical Chemistry C, 117, 8231–8240 (2013). (IF = 4.81)

2. Presentations relevant to the project:

[GV_1] G. N. Vayssilov, H. A. Aleksandrov, P. St. Petkov "Application of Computational Chemistry for Investigation the Structure and Properties of Heterogeneous Catalysts" (invited) Humboldt kolleg "New Prospects for Science and Education in the MENA region", Marrakech, Morocco, 2012

[GV_2] G. N. Vayssilov, P. St. Petkov, H. A. Aleksandrov, G. P. Petrova (plenary) "Understanding and predicting the structure and properties of nanostructured ceria-based catalysts using density functional modeling" National conference of Bulgarian Catalytic Club, Sofia, 2012

[GV_3] G. N. Vayssilov, P. St. Petkov, H. A. Aleksandrov, G P. Petrova, S. K. Kolev "Computational modeling of the structure and dynamics of nanosized systems and surfaces" PRACE Workshop "HPC Approaches in Life Sciences and Chemistry", Sofia, Bulgaria, 2012

[GV_4] Georgi N. Vayssilov, Petko St. Petkov, Hristiyan A. Aleksandrov, Valentin Valtchev "Evaluation of the relative stability of defect sites in zeolites by periodic density functional calculations" (invited) 1st Europe-Asia Zeolite Conference, Macao, January 2013.

[GV_5] Georgi Vayssilov, Petko Petkov, "Density Functional Modeling of the Structure and Dynamics of Transition Metal Clusters and Complexes in Zeolites", International Workshop Zeolites - Prospects and Challenges, May 2013, Caen, France (invited talk).

[GV_6] Georgi N. Vayssilov, "Density functional modeling of catalytic surfaces and nanoparticles" (invited) The Second International Conference on "Research to Applications & Markets", June 2013, Sousse, Tunisia.

[PP_1] Petko St. Petkov, "Spectroscopic features of adsorbates in MOFs - Computational modeling", 3th Annual congress of Nano science and technology, September 26-28 2013, Xian, China

[HA_1] Hristiyan Aleksandrov, "Computational modeling of the influence of surface H and/or subsurface C atoms on hydrogen absorption capacity of Pd nanoparticles", 3th Annual congress of Nano science and technology, September 26-28 2013, Xian, China

[GV_7] Georgi Vayssilov, "Modeling of catalytic surfaces and nanoparticles"

3th Annual congress of Nano science and technology, September 26-28 2013, Xian, China

[GV_8] Georgi Vayssilov, "Computational Studies of Structure and Properties of Surface Species on Ceria", Seminar at ETH Zurich, March 2013, Zurich, Switzerland.

[GV_9] Georgi Vayssilov, "Adsorbents and Catalysts as Studied by Computational Chemistry Methods", Seminar at UOP company, May 2013, Chicago, USA.

[GV_10] Georgi Vayssilov, "Computational modeling of catalysts", Seminar at University of Chicago, May 2013, Chicago, USA.

[GV_11] Petko Petkov, "Modeling of the adsorption properties of porous materials containing metal ions", Seminar at Beijing Computational Science Research Center, September 2013.

[GV_12] Hristiyan Aleksandrov, "Transformations of hydrocarbons on transition metal surfaces and nanoparticles", Seminar at Beijing Computational Science Research Center, September 2013.